Available online at www.sciencedirect.com

SciVerse ScienceDirect

Ceramics International 38 (2012) 3453–3458

CERAMICS INTERNATIONAL

www.elsevier.com/locate/ceramint

Plasma sprayed TiO_2: The influence of power of an electric supply on relations among stoichiometry, surface state and photocatalytic decomposition of acetone

Pavel Ctibor [a,*], Václav Štengl [b], Igor Píš [c], Tatiana Zahoranová [c], Václav Nehasil [c]

[a] Institute of Plasma Physics, ASCR, Za Slovankou 3, 182 00 Praha 8, Czech Republic

[b] Institute of Inorganic Chemistry, ASCR, Husinec-Rez, 250 68, Czech Republic

[c] Department of Surface and Plasma Science, Faculty of Mathematics and Physics, Charles University, V Holesovickach 2, 180 00 Praha 8, Czech Republic

Received 25 July 2011; received in revised form 21 December 2011; accepted 21 December 2011

Available online 31 December 2011

Abstract

The influence of input power on plasma sprayed coating was studied for a water-stabilized plasma spray torch (WSP®) and ceramic coatings formed from titanium dioxide (TiO_2). All other spray setup parameters were secured during the experiment with electric supply power as the only variable factor. Physical characteristics of the coatings were tested by means of Raman spectroscopy and X-ray photoelectron spectroscopy which are able to determine the stoichiometry and surface chemical composition of the coatings. Further, stoichiometry and surface states are crucial for the photocatalytic efficiency of the coatings. The photocatalytic procedure involved was UV-induced decomposition of acetone. Links between the tested features are drawn. The lower supply power used during the spraying of TiO_2 coating resulted in higher activity with respect to the photocatalytic point of view. Both the stoichiometry and surface composition are in the same time deviated from pure TiO_2.

Keywords: B. Spectroscopy; D. TiO_2; Plasma spraying; Photocatalysis

1. Introduction

When TiO_2 is irradiated with light of a wavelength lower than 420 nm (corresponding to 2.96 eV), an electron is excited from the valence band to the conduction band, and as a result, a hole is formed in the valence band. Photo-generated electrons and holes produce superoxide ions and hydroxyl radicals when they make contact with oxygen and water in the air i.e. decompose organic pollutants into CO_2, H_2O and harmless intermediate organic compounds by oxidation and reduction reactions of superoxide ions and hydroxyl radicals [1]. Generally, the photo-decomposition efficiency of organic pollutants in TiO_2 photocatalyst is influenced dramatically by the phase composition of TiO_2. Since the TiO_2 photocatalytic reaction is a surface reaction, surface states are important as regards the presence of the vacancies and impurities [2]. Plasma sprayed coatings with reasonable potential for various photocatalytic applications were reported. Coatings were sprayed on conventional as well as special substrates as foamed aluminum [3] or PET plates [4]. In other cases various approaches for an enhancement of the photoactivity were tested – spraying of nano-structured powders [5,6], a post-deposition treatment [7], HVOF spraying [8] or suspension plasma spray technique [9]. Direct comparison of the photo-activity of fine powder with specific surface in order of 10 m^2/g with ceramic coatings having real specific surface lower than 1 m^2/g is however problematic.

Notwithstanding a vast amount of literature published on photocatalysis, the effects of the oxidation state of TiO_2 coatings prepared by thermal spray on photocatalytic activity have not been thoroughly addressed. It is well known that thermal spray TiO_2 coatings are easily reduced due to the high temperature nature of the process, with the stoichiometry being a function of process parameters.

It is also known that the oxidation state of titanium plays a crucial role in photocatalytic reactions [7]. The formation of non-stoichiometric and oxygen-deficient lattice in rutile TiO_2 is due to formation of structural defects. The defects are mostly formed in the particles at high temperatures near the melting

* Corresponding author. Tel.: +42 266053717; fax: +42 286586389.
E-mail address: ctibor@ipp.cas.cz (P. Ctibor).

0272-8842/$36.00
doi:10.1016/j.ceramint.2011.12.058

point and are retained in the rapidly solidified layers. Since plasma used for spraying is a strong UV-light source, the photogenerated holes can yield to a formation of surface-bound hydroxyl groups, which are oxidizing agents and play important roles in photocatalytic reactions [3].

The structure, chemical state of the surface and coating morphology are influenced in plasma spraying process by various set-up parameters, among them the supply power is one of the most easily adjustable. The interconnection of these factors with the photocatalytic activity is a rather new task in the field of plasma spraying. Our target in the present paper is to evaluate the role of the power of an electric supply [10] onto photocatalytic activity of TiO_2-based coatings produced using atmospheric plasma spraying done by the water-stabilized plasma spray system.

2. Experimental

A description of the plasma spray procedure, power supplies employed and a feedstock powder was already published [10]. The power supply used for production of the here mentioned coatings was a high frequency converter type PL180WP (Bekaert Advanced Coatings Nv, Deinze, Belgium). It was used for plasma spraying on two markedly different levels of electric current – 350 A and 500 A. Corresponding powers were 100 and 150 kW.

The details concerning spraying set-up are summarized in Table 1.

As a feedstock powder for spraying natural rutile TiO_2 with sizes from 63 to 125 μm (mean size 94 μm) was used. This spray feedstock was prepared by a conventional crushing and sieving processes. It was fed by compressed air into the plasma stream, at a feeding distance (FD), which melts and accelerates the powder towards the surface of the substrate, placed at a spray distance (SD) downstream. Air was used as a powder feeding gas at pressure 2.5 bar and flow rate 3.25 slpm.

For a comparison, another natural rutile TiO_2 plasma sprayed sample (labeled U1) was included in the present study. Its main difference from the coatings sprayed by various power levels was that its feedstock has the size distribution from 100 to 170 μm. It consists of rutile phase. Here, because of larger particle size, the power was set as 154 kW, i.e. near the available maximum of the used power supply – classical thyristor controlled rectifier (Skoda, Czech Republic). Basic characterization of the coatings sprayed with two levels of the power of an electric supply was provided earlier [10]. Their additional characterization, associated closely with the photoactivity, is described in this paper.

Table 1
Parameters used for spraying.

Parameter	Value
Feeding distance, FD [mm]	56
Spray distance, SD [mm]	400
Feeding nozzle diameter [mm]	3
Feeding gas	Air
Powder size [μm]	63–125

X-ray diffraction (XRD) was performed on SIEMENS D500^{TM} theta-2theta Bragg–Brentano diffractometer, using cobalt K-alpha radiation, in order to gain information about the phases present within the feedstock powder and coatings.

Raman spectroscopy was performed using a Lambda Solutions P1 apparatus – laser wavelength 785 nm, objective magnification 50×, integration time 25 s. The surface of the coating was polished before the test.

The surface chemical composition of the coatings was measured by X-ray Photoelectron Spectroscopy. Experiments were carried out in an ultra-high vacuum chamber with a base pressure lower than 5×10^{-7} Pa. XPS experiments were performed using an Omicron EA 125 multichannel hemispherical analyzer with Al–K-alpha line (1486.6 eV) as a primary photon source. To exclude charging effects during the XPS measurements, photoelectron binding energies (EB) were corrected with reference to the Ti $2p_{3/2}$ peak of TiO_2, which was assumed to be positioned at a constant binding energy EB = 458.8 eV.

Photocatalytic decomposition of acetone was tested and the addressed coatings were compared with a reference sample U1. Kinetics of the photocatalytic degradation of gaseous acetone was measured by using a self-constructed stainless steel photoreactor [11] with a fluorescent lamp Narva LT8WT8/073BLB, i.e. a black lamp with 365 nm wavelength and input power 8 W (light intensity 6.3 mW/cm^2). Gas concentration was measured with the use of a quadrupole mass spectrometer JEOL JMS-Q100GC and a gas chromatograph Agilent 6890 N. A high-resolution gas chromatography column (19091P-QO4, J&W Scientific) was used. The sample from the reactor was taken via a sampling valve at time intervals of 2 h. The reactor of the total volume of 3.5 l was filled with oxygen using 1 L/min flow rate. The reactor internal space was thermostated at 35 °C and the dose of acetone applied by means of a Hamilton syringe through a needle and septum.

Porosity was measured by image analysis technique and the surface roughness by the Surtronic 3P (Taylor Hobson, UK) using contact technique. For an image analysis of light micrographs the software Lucia G (Lab. Imaging, Czech Rep.) was used. Reported values are averages from 10 frames analyzed at 250× magnification.

3. Results

X-ray diffraction pattern of the 350A and 500A coatings is shown in Fig. 1. The only phase detected is rutile. Also the reference coating U1 consists only of rutile phase. A certain loss of oxygen stoichiometry accompanies the anatase–rutile phase transformation in the plasma jet [12], but only seldom is detected by XRD.

Raman spectra are shown in Fig. 2. In the case of anatase, the bands corresponding to the Raman active fundamental modes are recorded at 518 cm^{-1} (A and B, unresolved) and 645 cm^{-1} [13]. The intensity of the peaks corresponding to anatase is very low for both samples (arrows in Fig. 2), being slightly higher for

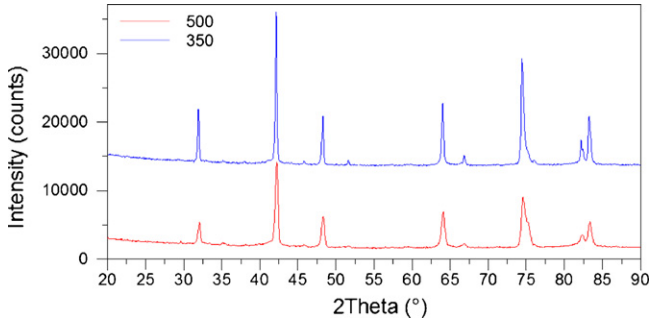

Fig. 1. X-ray diffraction pattern of the coatings 350 A (top) and 500 A (bottom).

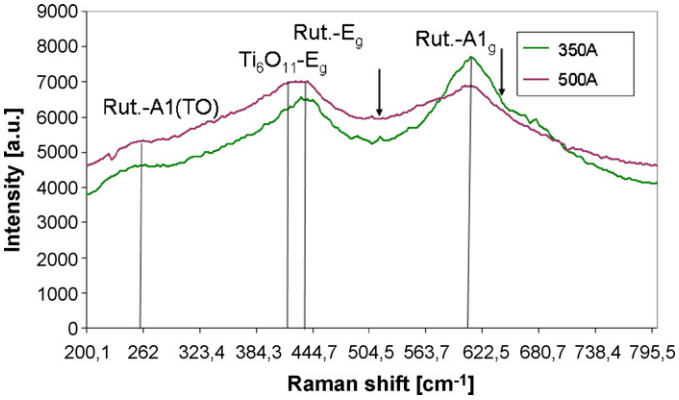

Fig. 2. Raman spectra of the coatings sprayed using 350 A current and 500 A current.

the 350A coating. Here the peak corresponding to smaller Raman shift is visible and the peak corresponding to larger Raman shift overlaps with $A1_g$ rutile peak. As for rutile, the spectra presented in Fig. 2 show two of the Raman active modes, respectively, at 440 cm^{-1} (E_g) and 610 cm^{-1} ($A1_g$) [13], elsewhere matched with 447 cm^{-1} (E_g) and 612 cm^{-1} ($A1_g$) [14]. The broad 2 g multiple peak at approximately 255 cm^{-1} results from a second order process [13].

Fig. 3 shows an example of the microstructure of 350A coating [10] taken as a light microscope on polished cross

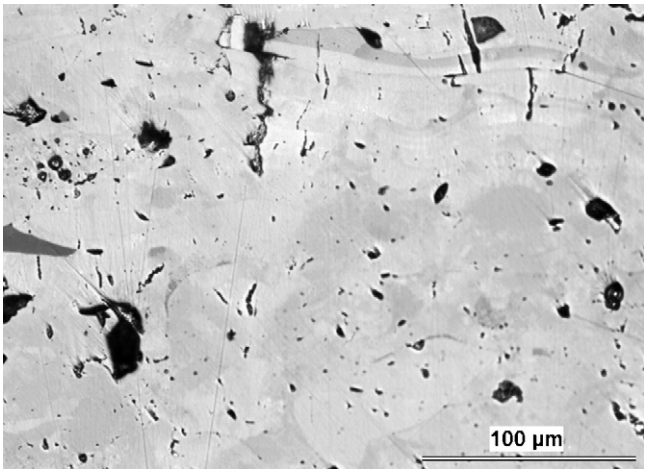

Fig. 3. An example of the microstructure of 350A coating [10]; light microscope; polished cross section.

section. Porosity is black. Splats are visible namely in the upper part of the image.

Fig. 4 displays kinetics of the UV-induced photocatalytic process. A decomposition of acetone is visible in the left graph whereas a simultaneous carbon dioxide augmentation in the right graph. Faster decrease of acetone concentration and at the same time faster increase of the CO_2 as a main reaction product means higher photocatalytic activity. Samples sprayed at current levels of 350 A and 500 A are compared with a reference sample U1.

XPS spectra of the U1 reference coating are displayed in Fig. 5 and compared with the 350A and 500A coatings. The almost identical Ti2p spectra, as far as the shape is concerned (Fig. 5a), showed that Ti^{4+} state dominated at the coating surfaces. On the contrary, O1s peaks (Fig. 5b) appeared to be different. They consisted of the main peak with the BE = 530.0 eV and states at the BE about 532.5 eV. The former peak corresponds to the Ti–O in TiO_2 and the higher binding energy states can be attributed to hydroxyl groups chemisorbed on the surfaces of the samples [3,15,16]. Both 350A and 500A

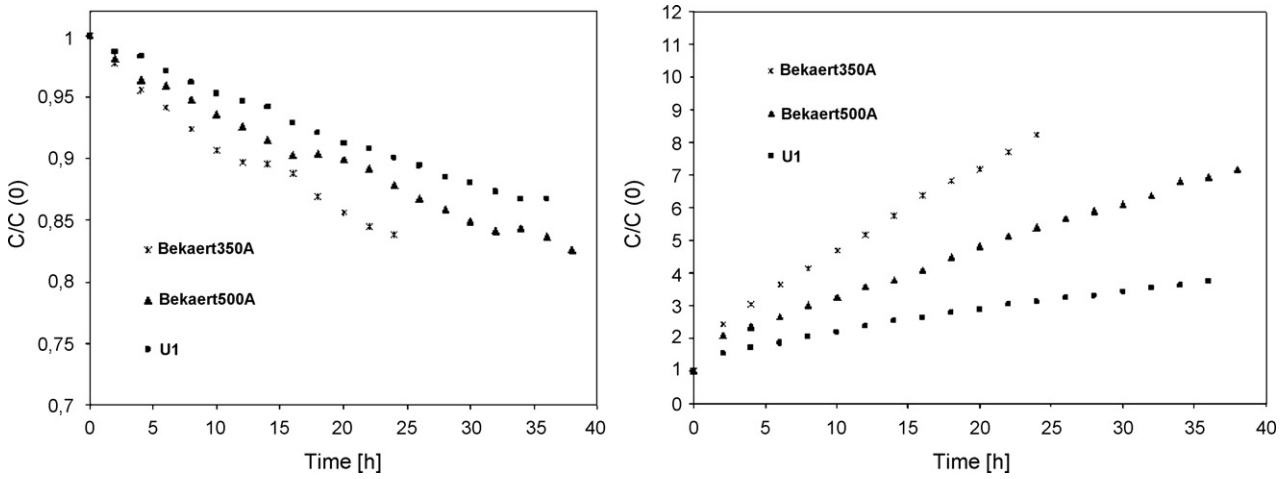

Fig. 4. Kinetics of the photocatalytic decomposition of acetone (left) and kinetics of the carbon dioxide augmentation.

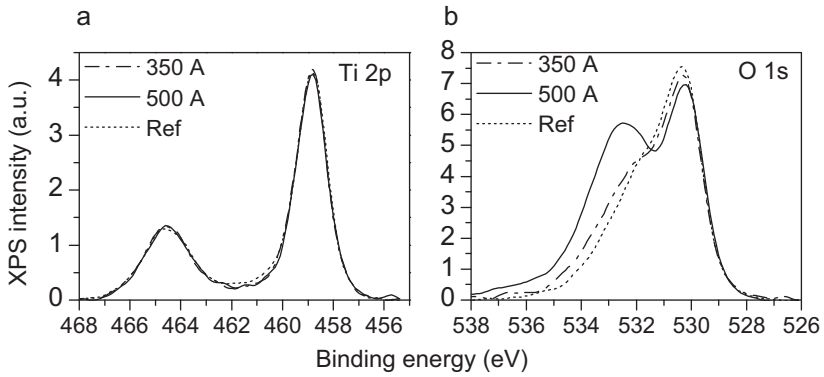

Fig. 5. Ti 2p (a) and O1s (b) XPS spectra of the WSP sprayed TiO_2 coatings using 350 A current, 500 A current and of the reference coating U1.

revealed higher amount of the –OH groups in comparison with the reference coating U1.

The N1s XPS peaks, Fig. 6, with maxima between 400.7 and 401.0 eV correspond to a structure with interstitial nitrogen (called also N-TiO_2) [17,18] coming from the ambient air surrounding the plasma. The interstitial nitrogen atoms can make the band-gap narrower [19,20], as confirmed by our bandgap estimation – see below, and the N-doping also promotes the formation of O-vacancy [20]. By this way a photocatalytic response is influenced by a simultaneous presence of a band level associated with O-nonstoichiometry and a band level associated with N-interstitials. This together with an existence of anatase in predominantly rutile coatings makes the photocatalytic action very complex [20,21].

Porosity and surface roughness data are summarized in Table 2. Porosity was measured by image analysis technique and its values varied around 4%, being highest for 350A coating and lowest for 500A coating. Both surface roughness parameters are highest for the reference sample U1 because of the large powder particles used for this coating.

4. Discussion

Concerning the Raman spectroscopy, for both 350A and 500A coatings the E_g peak of rutile (440 cm^{-1}) is broader and contains a sub-peak red-shifted to 420 cm^{-1}. Concerning this rutile red shift, oxygen deficiency appears to be the origin of this effect [13]. As for the exact extent of this non-stoichiometry, it is difficult to precise it because dark Ti suboxides are Raman-silent [13]. Normally, the crystal structure of a Magneli compound, such as Ti_4O_7, is built from successive blocks of rutile TiO_2, which are separated by two-dimensional shear planes to form Ti_4O_7. In our case, this E_g peak (see Fig. 2) is described as Ti_6O_{11} [22], however also Ti_4O_7-corresponding peak was reported at the same wave-number position [23]. Our plasma sprayed 350A and 500A coatings seem to contain certain quantity of Ti_4O_7/Ti_5O_9 in rutile matrix.

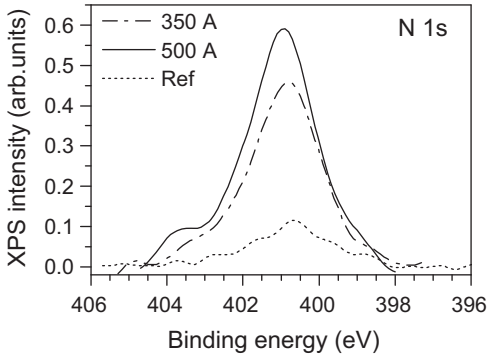

Fig. 6. N1s peak from the XPS spectra of the TiO_2 coatings using 350 A current, 500 A current and of the reference coating U1.

The intensity of the rutile $A1_g$ peak is higher for the 350A coating whereas the intensity of the rutile E_g is higher for the 500A coating (see Fig. 2). This fact could be associated with a preferential orientation (texture), however only for a film with very well defined impact and reflection angle of the radiation exhibiting Raman scattering on the surface, which is not at all the case of plasma sprayed coatings with cracks and pores opened to the surface (even after polishing).

Concerning the samples sprayed at 350 A and 500 A we see that the lower current level (i.e. power level) leads to higher photocatalytic activity (see Fig. 4). The band gap estimation of the coatings sprayed using 350 A current and 500 A current was reported earlier [10]. Both coatings exhibited band gap energy 2.85 eV and the reference coating U1 has also the same energy (while rutile has higher band gap energy ~3.0 eV). The lamp used for an illumination at the photocatalytic test has maximum intensity at 3.40 eV and its whole spectrum lies between 3.0 and 3.7 eV. The whole energy of the lamp radiation was absorbed by all three coatings. The Ti^{3+} ions from the reduced surface migrate to the bulk [13] where they occupy interstitial sites and the presence of adjacent Ti^{3+}–Ti^{4+} ions in the lattice is responsible for the dark blue color of the coatings.

Table 2
Structural characteristics.

Sample	350A	500A	U1
Porosity [%]	5.1 ± 1.0	3.2 ± 1.1	4.0 ± 1.4
Roughness R_a [μm]	13.7 ± 0.6	13.2 ± 1.2	19.3 ± 1.2
Roughness $R_{y\ max}$ [μm]	129.9 ± 11.0	109.6 ± 9.3	147.6 ± 20.9

XPS tests showed that the Ti2p spectra are the same for all three investigated coatings (see Fig. 5a). The O1s XPS spectra showed a relative amount of –OH groups on the coating surfaces. The presence of –OH groups is usually considered as an indicator of enhanced photoactivity [3,16,24]. The intensity variation concerning the N1s peak is associated with a reactivity of the powder particles. The reference powder, used for U1 coating spraying, with the coarser size provides smaller surface for the superficial reaction with the air atmosphere. The N1s peak is for the 500A coating higher than for the 350A coating because of higher particles temperature in the plasma [10] and correspondingly higher thermally promoted diffusion of the nitrogen inside the TiO_2.

As published earlier [10], the coating produced using lower power 100 kW (350 A) was more porous. Its porosity was $5.1 \pm 1.0\%$, whereas for 500A coating the porosity was only $3.2 \pm 1.1\%$. The higher porosity means larger contact area with the acetone during the photocatalytic test. The coating 350A has highest porosity, medium roughness (c.f. Table 2) and some–OH groups and interstitial N-atoms on the surface. The coating 500A has lowest porosity, lowest roughness (c.f. Table 2) but high quantity of –OH groups and interstitial N-atoms on the surface. The reference coating U1 has medium porosity, very high roughness (c.f. Table 2) but nearly no –OH groups on the surface and also no nitrogen incorporated. The photocatalytic efficiency is in this order: 350A, 500A, U1. We see that the photocatalytic efficiency arises from a combination of structural parameters as porosity and surface roughness with chemical parameters as presence of hydroxyl groups on the surface and presence of interstitial nitrogen atoms. The best coating from this viewpoint – 350A – represents a compromise between both these types of parameters.

5. Conclusions

Plasma sprayed coatings were prepared using TiO_2 rutile feedstock at two markedly different levels of the torch current which represent a change in the electric power used for plasma heating. Resulting coatings were used for photocatalytic decomposition of acetone induced by UV-light. Raman spectroscopy indicated presence of oxygen-deficiency on the surface. The studied coatings, including the reference coating, exhibit a complicated photocatalytic behavior based on presence of a band level associated with O-nonstoichiometry with a band level associated with N-interstitials. The associated physical background is more complex than for pure rutile TiO_2. This character is an inherent feature of atmospheric plasma sprayed coatings with oxygen-deficient surface including interstitial nitrogen atoms. Moreover, structural factors as porosity and roughness are much higher than is usual in i.e. thin films and must by taken into account. The photoactivity was best for the low-power sprayed coating labeled ''350A''. In a combination with its sufficient mechanical quality, which is acceptably maintained also when the spray power is diminished [10], the coatings sprayed with low power level are economically advantageous from the production viewpoint. They are suitable for self-supported functional layers in photocatalytic applications.

Acknowledgments

The spraying and photocatalytic testing was supported by the Grant Agency of the Academy of Sciences of the Czech Republic (project no. IAAX00430803). The XPS study was supported by the research program MSM 0021620834 financed by the Ministry of Education of the Czech Republic. I. Píš thanks also to the Grant Agency of the Czech Republic (grant no. 202/09/H041) for the research support.

References

[1] A. Fujishima, T. Inoue, K. Honda, Competitive photoelectrochemical oxidation of reducing agents at the titanium dioxide photoanode, Journal of the American Chemical Society 101 (1979) 5582–5588.
[2] J.-M. Herrmann, Heterogeneous photocatalysis fundamentals and applications to the removal of various types of aqueous pollutants, Catalysis Today 53 (1999) 115–129.
[3] H. Chen, S.W. Lee, T.H. Kim, B.Y. Hur, Photocatalytic decomposition of benzene with plasma sprayed TiO_2-based coatings on foamed aluminum, Journal of the European Ceramic Society 26 (2006) 2231–2239.
[4] T. Kanazawa, A. Ohmori, Behavior of TiO_2 coating formation on PET plate by plasma spraying and evaluation of coating's photocatalytic activity, Surface & Coatings Technology 197 (2005) 45–50.
[5] H. Lee Ch Choi, C. Lee, H. Kim, Photocatalytic properties of nano-structured TiO_2 plasma sprayed coating, Surface & Coatings Technology 173 (2003) 192–200.
[6] F.-L. Toma, G. Bertrand, D. Klein, C. Meunier, S. Begin, Development of photocatalytic active TiO_2 surfaces by thermal spraying of nanopowders, Journal of Nanomaterials (2008), article ID 384171.
[7] J. Colmenares-Angulo, S. Zhao, C. Young, A. Orlov, The effects of thermal spray technique and post-deposition treatment on the photocatalytic activity of TiO_2 coatings, Surface & Coatings Technology 204 (2009) 423–427.
[8] M. Bozorgtabar, M. Rahimipour, M. Salehi, Novel photocatalytic TiO_2 coatings produced by HVOF thermal spraying process, Materials Letters 64 (2010) 1173–1175.
[9] S. Kozerski, F.-L. Toma, L. Pawlowski, B. Leupolt, L. Latka, L.-M. Berger, Suspension plasma sprayed TiO_2 coatings using different injectors and their photocatalytic properties, Surface & Coatings Technology 205 (2010) 980–986.
[10] P. Ctibor, M. Hrabovský, Plasma sprayed TiO_2: the influence of power of an electric supply on particle parameters in the flight and character of sprayed coating, Journal of the European Ceramic Society 30 (2010) 3131–3136.
[11] P. Ctibor, V. Štengl, F. Zahálka, N. Murafa, Microstructure and performance of titanium oxide coatings sprayed by oxygen-acetylene flame, Photochemical and Photobiological Sciences 10 (2011) 403–407.
[12] R.S. Lima, C. Moreau, E. Garcia, P. Miranzo, M.I. Osendi, Development of HVOF-sprayed nanostructured TiO_2 coatings for high temperature applications, in: E. Lugscheider (Ed.), Thermal Spray Crossing Borders – Proc. of the Intl. Thermal Spray Conf. 2008, pp. 774–778.
[13] T.D. Robert, L.D. Laude, V.M. Geskin, R. Lazzaroni, R. Gouttebaron, Micro-Raman spectroscopy study of surface transformations induced by excimer laser irradiation of TiO_2, Thin Solid Films 440 (2003) 268–277.
[14] A. Orendorz, A. Brodyanski, J. Losch, L.H. Bai, Z.H. Chen, Y.K. Le, C. Ziegler, H. Gnaser, Phase transformation and particle growth in nano-crystalline anatase TiO_2 films analyzed by X-ray diffraction and Raman spectroscopy, Surface Science 601 (2007) 4390–4394.
[15] T.K. Sham, M.S. Lazarus, X-ray photoelectron spectroscopy (XPS) studies of clean and hydrated TiO_2 (rutile) surfaces, Chemical Physics Letters 68 (2–3) (1979) 426–432.
[16] M. Vijay, P.V. Ananthapadmanabhan, K.P. Sreekumar, Evolution of photocatalytic properties of reactive plasma processed nano-crystalline titanium dioxide powder, Applied Surface Science 255 (2009) 9316–9322.

[17] H. Shen, L. Mi, P. Xu, W. Shen, P.-N. Wang, Visible-light photocatalysis of nitrogen-doped TiO_2 nanoparticulate films prepared by low-energy ion implantation, Applied Surface Science 253 (2007) 7024–7028.
[18] F. Napoli, M. Chiesa, S. Livraghi, E. Giamello, S. Agnoli, G. Granozzi, G. Pacchioni, C. Di Valentin, The nitrogen photoactive centre in N-doped titanium dioxide formed via interaction of N atoms with the solid. Nature and energy level of the species, Chemical Physics Letters 477 (2009) 135–138.
[19] Y. Nakano, T. Morikawa, T. Ohwaki, Y. Taga, Band-gap narrowing of TiO_2 films induced by N-doping, Physica B 376–377 (2006) 823–826.
[20] F. Dong, W. Zhao, Z. Wu, S. Guo, Band structure and visible light photocatalytic activity of multi-type nitrogen doped TiO_2 nanoparticles prepared by thermal decomposition, Journal of Hazardous Materials 162 (2009) 763–770.
[21] C. Cantau, T. Pigot, J.C. Dupin, S. Lacombe, N-doped TiO_2 by low temperature synthesis: Stability, photo-reactivity and singlet oxygen formation in the visible range, Journal of Photochemistry and Photobiology A: Chemistry 216 (2010) 201–208.
[22] A. Skopp, N. Kelling, M. Woydt, L.-M. Berger, Thermally sprayed titanium suboxide coatings for piston ring/cylinder liners under mixed lubrication and dry-running conditions, Wear 262 (2007) 1061–1070.
[23] X. Li, A. Zhu, W. Qu, H. Wang, R. Hui, L. Zhang, J. Zhang, Magneli phase Ti_4O_7 electrode for oxygen reduction reaction and its implication for zinc-air rechargeable batteries, Electrochimica Acta 55 (2010) 5891–5898.
[24] E. Pelizzetti, C. Minero, Mechanism of the photo-oxidative degradation of organic pollutants over TiO_2 particles, Electrochimica Acta 38 (1) (1993) 47–55.